WATER RESOURCES RESEARCH, VOL. 50, 246–256, doi:10.1002/2013WR014718, 2014

Groundwater remediation using the information gap decision theory

D. O'Malley[1] and V. V. Vesselinov[1]

Received 12 September 2013; revised 17 December 2013; accepted 19 December 2013; published 10 January 2014.

[1] One of the challenges in the design and selection of remediation activities for subsurface contamination is dealing with manifold uncertainties. A scientifically defensible decision process demands consideration of the uncertainties involved. A nonprobabilistic approach based on information gap (info-gap) decision theory is employed to study the robustness of alternative remediation activities. This approach incorporates both parametric and nonparametric (conceptual) uncertainty in predicting contaminant concentrations that are effected by natural processes and the remediation activities. Two remedial scenarios are explored to demonstrate the applicability of the info-gap approach to decision making related to groundwater remediation.

Citation: O'Malley, D., and V. V. Vesselinov (2014), Groundwater remediation using the information gap decision theory, *Water Resour. Res.*, *50*, 246–256, doi:10.1002/2013WR014718.

1. Introduction

[2] Remediation of anthropogenic subsurface contamination is a significant challenge facing the world [*NRC*, 2013; *Rügner et al*., 2006]. For many contaminated sites, the available data and documentation of various parameters characterizing contaminant releases such as magnitude, timing, spatial distribution, and contents are limited [*Pierce et al*., 2009]. There is also limited site information about the geological, hydrological, and biogeochemical conditions; information that is necessary for a complete understanding of contaminant transport and its impact on the environment. It is well recognized that the environmental management of contaminated sites requires robust decision analysis tools based on risk assessment and taking into account existing budget constraints [*NRC*, 2013, 1999]. The site and technological complexities require data-driven and model-driven decision analyses for environmental management in which limited site information and physics models are coupled to perform scientifically defensible and legally sound risk assessment and decision analysis. However, such theoretical methodologies and computational tools for subsurface contaminant remediation that explicitly account for lack of or limited knowledge about the governing process and their parameters are often insufficient [*Agostini et al*., 2009a, 2009b; *Argent et al*., 2009; *Deeb et al*., 2011; *Jordan and Abdaal*, 2013; *NRC*, 1999; *Tartakovsky*, 2007; *Bolster et al*., 2009].

[3] A crucial component of any decision analysis for remediation of contaminated sites is predicting the future fate of the contaminant plume. However, predicting contaminant concentrations in the subsurface is fraught with uncertainties. Typically, there is uncertainty in present size, shape, and location of a contaminant plume. There is also uncertainty in the rates at which the contamination plume will evolve in time. Frequently, the plume fate is controlled by an advective velocity field, biogeochemical reaction rates, and dispersion coefficients or tensors as well as their temporal and spatial variations. As a result, making decisions related to contaminant remediation is challenging as well.

[4] Severe parametric uncertainties make it difficult to make accurate model predictions going forward. They may make it extremely difficult to effectively characterize the uncertainties probabilistically. In a high-dimensional space with heavy-tailed probability distributions, it can be challenging to obtain a representative sample. There has been progress in reducing the computational cost of this process [cf. *Tonkin and Doherty*, 2009; *Laloy and Vrugt*, 2012], but it remains computationally demanding. The effect of this is that important events in the tails can be overlooked.

[5] On top of parametric uncertainties, there are model uncertainties related to conceptual assumptions. These arise from a lack of comprehensive understanding about the processes governing the contaminant migration in the subsurface and their upscaled representation in predictive models. Frequently, the conceptual uncertainties are handled by defining a range of alternative models representing site conditions and governing physical processes [*Ye et al*., 2004]. However, some or all of the proposed site models might be inadequate. Inadequate models may be able to represent existing site observations very well, but fail to make defensible predictions about future plume fate. As a result, even the best models may suffer from some degree of inadequacy [*Beven and Westerberg*, 2011]. Model uncertainty also creates additional problems for the probabilistic approach to parameter uncertainty. In particular, the models under consideration may not be sufficient to characterize the set of all possible outcomes. High-probability events may not be accounted for at all, and all the events that are accounted for could have a low cumulative probability.

[1]Computational Earth Science Group, Earth and Environmental Sciences Division, Los Alamos National Laboratory, Los Alamos, New Mexico, USA.

Corresponding author: D. O'Malley, Computational Earth Science Group, Earth and Environmental Sciences Division, Los Alamos National Laboratory, Los Alamos, NM 87545, USA. (omalled@lanl.gov)

0043-1397/14/10.1002/2013WR014718

[6] There are additional uncertainties (e.g., arising from observation or numerical computational errors, etc.). These will not be the focus of attention here. Observational uncertainties can be accounted for during the model selection and calibration phase which we do not consider. The model and parametric uncertainties under consideration are likely to dominate uncertainties associated with things like numerical errors.

[7] Owing to the multitude of uncertainties, model predictions are uncertain and may not provide sufficient support when making decisions about contaminant remediation strategies. In consequence, it is necessary to account for the prediction uncertainty in the decision process. There are numerous methods that have been designed to achieve this, e.g., *Caselton and Luo* [1992]; *Hipel and Ben-Haim* [1999]; *Bolster et al*. [2009]; *Reeves et al*. [2010]; and *Harp and Vesselinov* [2013].

[8] A good review of dealing with uncertainty in surface and subsurface hydrology is presented in *Montanari et al*. [2009]. Perhaps the most common approach to quantifying uncertainty is with probability and statistics [see e.g., *Delhomme*, 1979; *Dagan*, 1982; *Wagner and Gorelick*, 1987; *Abbaspour et al*., 1997; *Keating et al*., 2010]. In the presented setting, this approach could be applied, e.g., by associating probability distributions with each model parameter. A more intricate approach would be to associate a probability distribution with a class of models, and then associate probability distributions with each parameter for each model [*Neuman*, 2003; *Ye et al*., 2004; *Morales-Casique et al*., 2010; *Singh et al*., 2010]. The probabilistic approach is natural and powerful if the probability distributions are known [*Bedford and Cooke*, 2001], but this is often not the case. A common way to resolve this difficulty is to apply Bayes theorem with a uniform prior. The uniform prior is not ideal because there is no basis for its definition. However, Bayes theorem has the potential to overcome this limitation if enough data are available to make the posterior distribution converge to the true distribution. In subsurface transport data tend to be scarce, so this generally does not occur. Even if sufficient data are available to compute an accurate posterior, the result is often that nearly all of the probability is concentrated on a single model. Ideally this would happen because the most likely model is essentially correct, but it is also possible that the most likely model is merely less inadequate than the others.

[9] In practice, it is often problematic to formulate reasonable probability distributions for a multitude of parameters and/or models. In such cases, a nonprobabilistic approach may be used. The nonprobabilistic approaches do not require prior probabilistic information about uncertainty in parameters and models. Here, we present a nonprobabilistic analysis of remedial alternatives related to groundwater contamination based on information gap (info-gap) decision theory [*Ben-Haim*, 2006]. In the context of contaminant remediation, this approach essentially looks for the worst-case scenario as a function of the unknown horizon of uncertainty. Multiple models fit naturally into this paradigm through its definition of the decision robustness which will be discussed in greater detail. Early applications of info-gap theory to environmental management were carried out in *Hipel and Ben-Haim* [1999] and *Levy et al*. [2000]; watershed and forest (respectively) management under severe uncertainty were considered. Building on this work, info-gap has also been applied to flood risk management decisions [*Hine and Hall*, 2010] and revegetation strategies after wildfires [*McCarthy and Lindenmayer*, 2007]. Further research demonstrated the utility of using the info-gap approach to ecological experimental design [*Fox et al*., 2007]. Recently, info-gap has been applied to contaminant remediation by considering uncertainty in the source of the contamination [*Harp and Vesselinov*, 2013].

[10] We build upon *Harp and Vesselinov* [2013] by considering a more extensive uncertainty model that includes parametric uncertainty in the dispersion as well as model uncertainty (including in the source of the contamination) as well as considering two remediation alternatives that have different costs associated with their implementation. The results are analytical in nature. Though the physics-based model that we use is fairly simple, more complex models are included within the info-gap uncertainty model. The model was chosen not because of the limitations of the info-gap approach, but to provide a better demonstration of a relatively novel method for decision analysis which otherwise may be difficult to understand. More complex physics or uncertainty models may be analytically intractable, but computational methods can be used when this occurs. The computational cost has the potential to be very high if there are many parameters or many local extrema. However, it is generally less expensive than Bayesian methods. This is because the entire parameter space does not need to be sampled—only an optimization routine must be performed.

2. Methodology

[11] Application of info-gap decision theory can be briefly summarized as:

[12] 1. Formulate "performance requirements" (i.e., "decision goals")

[13] 2. Construct an uncertainty model.

[14] 3. Determine the robustness to uncertainty: the maximum "horizon of uncertainty" up to which performance requirement will be satisfied.

[15] After these steps have been performed, the robustness to uncertainty can be used to inform a decision. The purpose of finding the robustness is to see how far the system can deviate from the nominal case (analogous to a point estimate in a probabilistic approach) before the performance requirement fails. When comparing remediation strategies, one that has greater robustness (requires more uncertainty before the performance requirement is not satisfied) would be seen as better. This is analogous in some ways to preferring a remediation strategy that has a smaller maximum likelihood of failure in a probabilistic approach, but the info-gap approach does not require the definition of any probabilities.

[16] When choosing a remediation strategy where the budget is the primary constraint, it is best to choose the strategy that provides the greatest robustness within the budget. When choosing a remediation strategy where the need for robustness is the primary constraint, it is best to choose the strategy that provides sufficient robustness at the lowest cost.

[17] In the context of contaminant remediation, formulating a performance requirement is often easy. Usually, the contaminant concentrations are required to be below some threshold such as a Maximum Concentration Limit (MCL) for drinking water supply (EPA, 2013, http://water.epa.gov/drink/contaminants/) at a point of compliance. Suppose for the demonstration purposes that the performance requirement is that the model predicted concentration, $\tilde{C}$, at a point of compliance at x_c for a given time range, (t_{c_0}, t_{c_1}), be below the threshold C_c. In the broadest case, the compliance time range can be from 0 to ∞; a narrower case, can be defined where t_{c_0} and t_{c_1} are certain moments of time in the future. Once the performance requirement is determined, the next step is to construct an uncertainty model.

[18] In info-gap decision theory, the uncertainty model depends on a parameter called the "horizon of uncertainty," which we will denote ϵ throughout. It is often desirable to make ϵ nondimensional, and we will employ this practice.

[19] Generally in an info-gap model, the most challenging step is determining the greatest horizon of uncertainty for which the performance requirement is guaranteed to be satisfied. The maximum horizon of uncertainty (or robustness) tells us how much uncertainty must be present before the performance requirement is not satisfied. When comparing two remediation strategies, it is prudent to choose the one that requires more uncertainty in order to fail (all else being equal). Determining the robustness may require complex analytical approaches or computationally demanding numerical exploration of parameter space within the horizon of uncertainty to find the worst (and best) possible model predictions within a given horizon of uncertainty.

[20] In hydrology and many other fields, it is common to "minimize uncertainty" when selecting models. That is, to choose a model or model parameters that minimize some objective function measuring the discrepancy between measurements and model predictions. The model/parameter selection process is outside the scope of this paper, and can be carried out using any number of methods.

[21] Below we will construct two alternative setups of the info-gap analyses with different levels of complexity; in each case, the robustness is estimated analytically. The first is an oversimplified model to demonstrate the info-gap process. The second uses a physics-based model of subsurface contaminant advection-reaction-diffusion.

3. Info-Gap Analyses

3.1. Illustrative Info-Gap Analysis

[22] To get a better understanding of an info-gap decision framework, consider a typical info-gap uncertainty model for a parameter p

$$\mathcal{P}(\epsilon)=\left\{p : \left|\frac{p-\tilde{p}}{\tilde{p}}\right| \le \epsilon\right\}, \epsilon \ge 0 \tag{1}$$

where $\tilde{p}$ is the "nominal" value of p, i.e., the p that would be used if only one p value could be considered. Here and henceforth $(\tilde{\cdot})$ is used to denote a "nominal" value, that is, a value considered to be representative of our current understanding of the site conditions and based on which a decision can be made. However, the amount of discrepancy between the "nominal" and "true" value for each parameter is unknown. In info-gap theory, one evaluates the robustness to the uncertainty around the nominal model. The info-gap analyses can be performed from a series of different nominal values which will provide more detailed estimation of decision uncertainties. This uncertainty model $\mathcal{P}(\epsilon)$ includes all values of p that are within a fractional error less than ϵ from $\tilde{p}$. Depending on the context, a different uncertainty model could be constructed that reflected a different understanding of the uncertainty involved.

[23] Suppose, again for demonstration purposes, that a simple linear model is used to predict the contaminant concentration $[M/L^3]$

$$C(x;p)=C_0-px \tag{2}$$

where $x>0$ is some lateral distance from the contaminant source $[L]$, and $p>0$ here represents a forcing parameter that causes contaminant migration $[M/L^4]$. The concentration at the source is C_0 $[M/L^3]$. The shape and size of the contaminant source is not considered and is irrelevant in this simple example. The value of p must be positive so that the concentration C $(x;\ p)$ declines with the traveled distance x away from the source (the source is at $x=0$).

[24] The maximum horizon of uncertainty (denoted $\hat{\epsilon}$) for which the performance requirement ($C(x_c;p) < C_c$, where x_c is the point of compliance) holds is

$$\hat{\epsilon}(\tilde{p})=\max\left\{\epsilon : \left[\max_{p\in\mathcal{P}(\epsilon)} C(x_c;p)\right] < C_c\right\} \tag{3}$$

[25] If the set that the maximum is taken over is empty, i.e., if $C(x_c;\tilde{p}) \ge C_c$, then by convention, $\hat{\epsilon}=0$. This can occur only if the nominal value does not satisfy the performance requirement (i.e., $\tilde{p} \le \frac{C_0-C_c}{x_c}$). Assume that the nominal value does satisfy the performance requirement. In order to determine $\hat{\epsilon}$, it is necessary to first compute

$$\max_{p\in\mathcal{P}(\epsilon)} C(x_c;p)=C_0-\max\left[0,(1-\epsilon)\tilde{p}\right]x_c \tag{4}$$

[26] Setting the maximum concentration equal to C_c and solving for ϵ, we obtain

$$\hat{\epsilon}(\tilde{p})=\frac{C_c-C_0+\tilde{p}x_c}{\tilde{p}x_c} \tag{5}$$

where it has been assumed that $C_0 > C_c$. Essentially what $\hat{\epsilon}$ tells us is the greatest tolerable relative error in p before the concentration at x_c exceeds the threshold, C_c. The robustness as a function of $\tilde{p}$ is plotted in Figure 1 under the assumption that $C_0=25;[M/L^3]$, $C_c=5;[M/L^3]$ and $x_c=10;[L]$.

[27] The same problem can be explored using the same linear model for the concentration, but with a more extensive uncertainty model. Let

$$\mathcal{F}(\epsilon)=\left\{C : \left|\frac{C(x_c;\cdot)-\tilde{C}(x_c;p)}{\tilde{C}(x_c;p)}\right| < \epsilon, \text{for some} \, p \in \mathcal{P}(\epsilon)\right\}, \epsilon \ge 0 \tag{6}$$

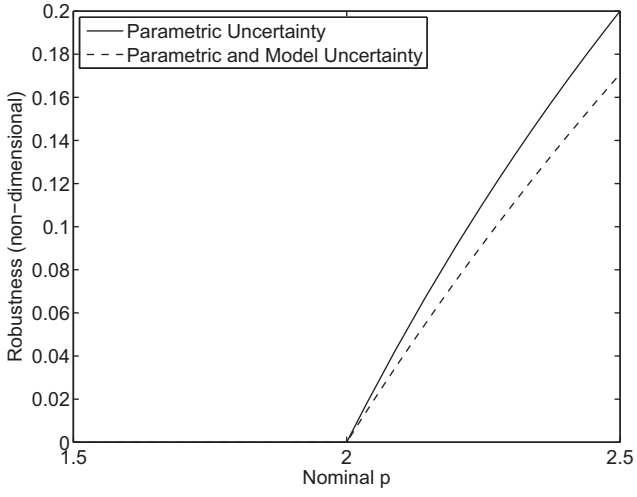

Figure 1. Robustness curves of the two info-gap models as a function of nominal p $(\tilde{p})$ with $C_0 = 25$, $C_c = 5$, and $x_c = 10$.

be a new uncertainty model that includes both parametric uncertainty and uncertainty in the functional form of the model; in the equation above, $C(x_c, \cdot)$ is a model prediction based on an implicit, unspecified model and set of model parameters (which may or may not include p), and $\tilde{C}(x_c; p)$ is a prediction based on equation (2) where p is within the ϵ horizon of uncertainty of $\tilde{p}$. Uncertainty in the functional form is included because $\mathcal{F}(\epsilon)$ includes functions (i.e., models for predicting the contaminant concentration $C(x_c, \cdot)$ at x_c) that do not have the functional form of equation (2). However, all the conceptual models need to be bounded within the info-gap uncertainty bound defined in equation (6). Note that the horizon of uncertainty, ϵ, is unknown, reflecting the fact that we do not know how much the nominal model errs.

[28] With this new uncertainty model, the robustness is given by

$$\hat{\epsilon}(\tilde{p}) = \max\left\{\epsilon : \left[\max_{C\in\mathcal{F}(\epsilon)} C(x_c)\right] < C_c\right\} \tag{7}$$

[29] Following a procedure similar to before, we first compute the inner maximum. This computation proceeds by first finding the value of $p \in \mathcal{P}(\epsilon)$ that maximizes $C_0 - p x_c$ which was previously determined to be $p = \max\{(1-\epsilon)\tilde{p}\}$ (from equation (2), making p as small as possible, makes the prediction as large as possible). From there, it is seen that the choice of $C(x;\cdot) \in \mathcal{F}(\epsilon)$ that maximizes the prediction is $C(x;\cdot) = (1+\epsilon)C(\tilde{x}; p)$. Therefore,

$$\max_{C\in\mathcal{F}(\epsilon)} C(x_c) = (1+\epsilon)(C_0 - \max[0, (1-\epsilon)\tilde{p}]x_c) \tag{8}$$

$$= (1+\epsilon)C_0 - \max[0, (1-\epsilon^2)\tilde{p}]x_c \tag{9}$$

where we have assumed that $C_0 > C_c/2$ (i.e., the concentration at the source is at least half the MCL) and $C_0 - \tilde{p}x_c \leq C_c$ (i.e., the nominal prediction of the concentration at the point of compliance is not above the MCL). Then we compute the outer maximum by setting the inner maximum equal to the MCL (C_c) and solving (taking the positive root)

$$\hat{\epsilon}(\tilde{p}) = \frac{\sqrt{C_0^2 + 4\tilde{p}x_c[C_c - C_0 + \tilde{p}x_c]} - C_0}{2\tilde{p}x_c} \tag{10}$$

[30] The robustness function associated with this setup is also plotted in Figure 1.

[31] Two interesting features are noted in Figure 1. First, as already discussed, the robustness is 0 for $\tilde{p} \leq 2 = \frac{C_0 - C_c}{x_c}$. This is because for $\tilde{p} \leq 2$, the nominal prediction is above the threshold. Hence failure to meet the performance requirement is expected, and there is no robustness. The second feature is that the robustness increases at a slower rate (with respect to $\tilde{p}$) when uncertainty in the functional form (conceptual model) is included. This is natural, because including uncertainty in the functional form accounts for the possibility of more things going wrong. That is, the use of the nominal parameter $\tilde{p}$ could be too high (making the prediction too low) and the linear model may be inadequate (perhaps further making the prediction too low). This info-gap model accounts for both possibilities whereas the first info-gap model only accounted for uncertainty in $\tilde{p}$. Consistent with the case of decision robustness (Figure 1), the maximum predicted concentration within a given horizon of uncertainty is higher when model uncertainty is included (Figure 2). Regardless of its simplicity, this info-gap analysis demonstrates the power of the proposed technique and the importance of incorporating model uncertainty in decision analyses. A more complicated model for predicting contaminant concentrations is applied for info-gap analysis in the next section.

3.2. Model-Based Info-Gap Analysis

[32] The model used in this section is the solution of the reaction-advection-diffusion partial differential equation (PDE)

$$\frac{\partial C}{\partial t} = -u\frac{\partial C}{\partial x} + D_x\frac{\partial^2 C}{\partial x^2} + D_y\frac{\partial^2 C}{\partial y^2} + D_z\frac{\partial^2 C}{\partial z^2} - \lambda C + \frac{I}{\theta} \tag{11}$$

on an infinite domain and the concentration is initially zero until the source I adds mass at $t = 0$ so that

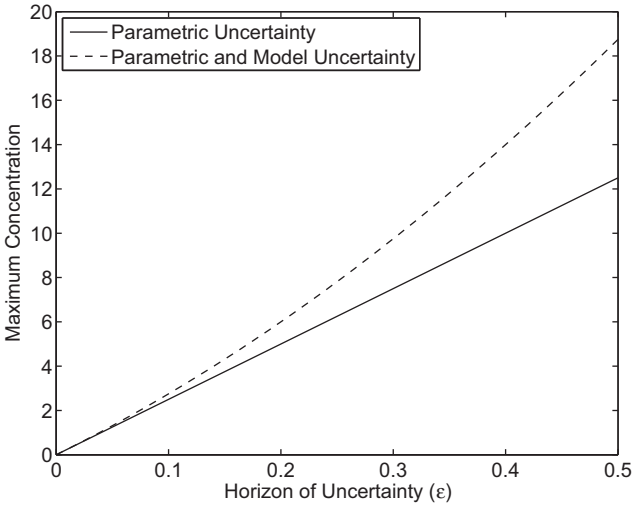

Figure 2. Maximum concentration as a function of horizon of uncertainty.

$$C(x,y,z,t)=\frac{\int_0^t\int_{\mathbb{R}^3} I(x',y',z',t-\tau)\exp\left[-\lambda\tau-\frac{(x-x'-u\tau)^2}{4D_x\tau}-\frac{(y-y')^2}{4D_y\tau}-\frac{(z-z')^2}{4D_z\tau}\right]d\mathbf{x}'\,\frac{d\tau}{\tau^{3/2}}}{8\pi^{3/2}\theta\sqrt{D_xD_yD_z}} \tag{12}$$

is the concentration of a contaminant at location $\mathbf{x}=(x,y,z)$ at time $t>0$, λ is a half-life decay constant (T^{-1}) representing the rate of zero-order biogeochemical reactions (if $\lambda=0$, there is no reaction), D_x, D_y, and D_z are dispersion coefficients (L^2/T) in the x, y, and z directions, respectively, u is an advective (linear) velocity (L/T) in the x direction, and θ is the porosity [−] [*Wang and Wu*, 2009]. $I(x,y,z,t)$ is an instantaneous contaminant source at $t=0$. Here, it can be represented as a Gaussian plume as present at time 0

$$I(x,y,z,t)=\frac{M(1-q)}{\sqrt{8\pi^3\sigma_x^2\sigma_y^2\sigma_z^2}}\exp\left(-\frac{(x-x_0)^2}{2\sigma_x^2}-\frac{(y-y_0)^2}{2\sigma_y^2}-\frac{(z-z_0)^2}{2\sigma_z^2}\right)\delta(t-0) \tag{13}$$

where M is the contaminant mass (M), q is the fraction of the contaminant mass that has been removed [−], (x_0, y_0, z_0) is the central location of the contaminant source (L), and σ_x, σ_y, σ_z are the standard deviations of the contaminant source concentration (L^2).

[33] After simplification, equation (12) reduces to

$$C(x,y,z,t)=\frac{M(1-q)\exp\left[-\lambda t-\frac{(x-x_0-ut)^2}{2(2D_xt+\sigma_x^2)}-\frac{(y-y_0)^2}{2(2D_yt+\sigma_y^2)}-\frac{(z)^2}{2(2D_zt+\sigma_z^2)}\right]}{\theta\sqrt{2\pi^3(2D_xt+\sigma_x^2)(2D_yt+\sigma_y^2)(2D_zt+\sigma_z^2)}} \tag{14}$$

where it is assumed that $z_0=0$ and there is a reflecting boundary at the top of the aquifer ($z=0$). The effect of this is that the concentration is doubled at every point since half of the contaminant mass is reflected across the plane $z=0$.

[34] Two alternative remedial actions can be represented using equation (14). The contaminant mass introduced in the subsurface M may have been reduced by different fractions q by some kind of remedial action such as pump-and-treat or source removal. The contaminant mass migrating in the subsurface may also be reduced by some in situ treatment which increases the reaction rate which is represented by increasing λ. This can be achieved by dispersing uniformly some biomass throughout the plume that enhances the contaminant decay. Both remedial actions are commonly applied for contaminant remediation of the subsurface.

[35] We wish to define an uncertainty model that explicitly incorporates uncertainty in the dispersion coefficients and implicitly incorporates uncertainty in the other parameters and the functional form of the concentration predictions. As was done with the simple linear model, this can be accomplished by combining two info-gap uncertainty models. One is for uncertainty in the dispersion coefficients, and the other expands on this to include uncertainty in the other parameters and the functional form. Uncertainty in the dispersion coefficients is captured via

$$\mathcal{U}(\epsilon)=\left\{(D_x,D_y,D_z):\left|\frac{D_\psi-\tilde{D}_\psi}{\tilde{D}_\psi}\right|<\epsilon, D_\psi\geq 0, \forall\psi\in\{x,y,z\}\right\}, \epsilon\geq 0 \tag{15}$$

[36] Broader uncertainty in the other parameters and uncertainty in the functional form is captured via

$$\mathcal{G}(\epsilon,t,\mathbf{x})=\left\{C:\left|\frac{C(\mathbf{x},t;\cdot)-\tilde{C}(\mathbf{x},t;\mathbf{D})}{\tilde{C}(\mathbf{x},t;\mathbf{D})}\right|<\epsilon,\forall\mathbf{x},\ \text{for some } \mathbf{D}=(D_x,D_y,D_z)\in\mathcal{U}(\epsilon)\right\}, \epsilon\geq 0 \tag{16}$$

where $\tilde{C}(\mathbf{x},t;\mathbf{D})$ is the nominal model prediction with dispersion coefficients given by $\mathbf{D}$, and $C(\mathbf{x},t;\cdot)$ are model predicted concentrations with models and parameters different from the nominal case. $\tilde{C}(\mathbf{x},t;\mathbf{D})$ is computed based on equation (14). The functional form of $C(\mathbf{x},t;\cdot)$ is neither known nor necessary for the info-gap analysis. So, for example, models that include heterogeneous parameters will be included in $\mathcal{G}(\epsilon,t,\mathbf{x})$ for $\epsilon>0$, and the degree of heterogeneity that is permitted will increase as ϵ increases. Many possible models exist within $\mathcal{G}(\epsilon,t,\mathbf{x})$, and it is impossible to enumerate them all. It is only necessary to compute the maximum predicted concentration over all elements of $\mathcal{G}(\epsilon,t,\mathbf{x})$ at $\mathbf{x}$ at time t for each horizon of uncertainty (ϵ). Note that this allows for uncertainty in parameters other than the dispersion coefficient (including λ and q which are important parameters characterizing potential alternative remedial actions). With the proposed info-gap uncertainty model (equation (16)) it is possible to take into account lack of knowledge about the magnitude of naturally occurring dispersion in the subsurface and how this lack of knowledge will impact the design of remedial activities (i.e., how much to increase λ and q through remedial activities without over achieving the performance goals).

[37] It is important to note equation (16) allows for application of alternative conceptual models (functional forms) for computation of contaminant concentrations; in fact, any functional form bounded by the info-gap uncertainty model equation (16) (i.e., enveloped between the best and worst predicted behavior based on equation (14) within equation (16)) is taken into account. For example, uncertainty in conceptual assumptions like non-Gaussian sources, non-Gaussian dispersion, nonzero-order reaction rates, nonstationary dispersion, etc. These aspects of the info-gap analysis are demonstrated for the case of Scenario 1 below.

[38] For any remedial activity, it is very important to account for budgetary constraints. It is assumed that there is some control over the biogeochemical reaction rate, but inducing an increase in the reaction rate comes with additional cost. As a function of the price, P_λ, the nominal reaction rate is

$$\tilde{\lambda}(P_\lambda)=\lambda_0+\max\left\{0,\frac{P_\lambda-S_\lambda}{I_\lambda}\right\};[1/\text{year}] \tag{17}$$

where S_λ is a start-up cost and I_λ is an incremental cost for increasing λ. Similarly, for the reduction of the introduced contaminant mass in the subsurface $\tilde{q}$,

$$\tilde{q}(P_q)=\max\left\{0,\frac{P_q-S_q}{I_q}\right\} \tag{18}$$

where P_q, S_q, and I_q are the price, the start-up cost, and the incremental cost associated with the fraction of the mass removed q. Sometimes P will be used denote either P_λ or P_q depending on which remediation technique is under consideration. All costs are left unitless. Here, the start-up costs (S_λ and S_q) represent the investment required to set the remedial system in place (e.g., drilling wells, building infrastructure, etc.). In some cases, the start-up costs may be equal to zero if the infrastructure is already in place. The incremental costs ($I_\lambda(\lambda-\lambda_0)$ and $I_q q$) are additional investments to increase contaminant mass reduction. The proposed methodology can be applied with much more complicated models for estimation of the price of the remedial activities.

[39] The performance requirement is that the concentration at a point of compliance located at $\mathbf{x}_c=(x_c,y_c,z_c)$ be below a threshold, C_c, at any time $t>0$ (compliance time range is $t_{c_0}=0$ and $t_{c_1}\to\infty$).

$$C(\mathbf{x}_c,t)<C_c,\forall t\geq 0 \tag{19}$$

[40] In our case, the maximum concentration $C(\mathbf{x}_c,t)$ will occur when the peak of the plume is the closest to the point of compliance.

[41] This enables the computation of the maximum horizon of uncertainty for which the threshold requirement (equation (19)) is not violated. If the nominal prediction at the point of compliance is above the threshold, then the robustness is zero. Otherwise,

$$\hat{\epsilon}(\mathbf{x}_c,t)=\max\left\{\epsilon\geq 0:\left(\max_{C\in\mathcal{G}(\epsilon,t,\mathbf{x}_c)}C(\mathbf{x}_c,t)\right)<C_c\right\}. \tag{20}$$

[42] Some calculus, algebra, and inspection (see Appendix A for more information) implies that the inner maximum occurs when $C(\mathbf{x}_c,t)=(1+\epsilon)\tilde{C}(\mathbf{x}_c,t;\mathbf{D}^*)$ with

$$D_x^*=\max\left\{0,(1-\epsilon)\tilde{D}_x,\min\left\{(1+\epsilon)\tilde{D}_x,\frac{(x_c-x_0-ut)^2-\sigma_x^2}{2t}\right\}\right\} \tag{21}$$

$$D_y^*=\max\left\{0,(1-\epsilon)\tilde{D}_y,\min\left\{(1+\epsilon)\tilde{D}_y,\frac{(y_c-y_0)^2-\sigma_y^2}{2t}\right\}\right\} \tag{22}$$

$$D_z^*=\max\left\{0,(1-\epsilon)\tilde{D}_z,\min\left\{(1+\epsilon)\tilde{D}_z,\frac{z_c^2-\sigma_z^2}{2t}\right\}\right\} \tag{23}$$

so the robustness (the outer maximum in equation (20)) is obtained by solving for ϵ in $(1+\epsilon)\tilde{C}(\mathbf{x},t;\mathbf{D}^*)=C_c$ when $\tilde{C}(\mathbf{x}_c,t;\mathbf{D}^*)<C_c$. When $\tilde{C}(\mathbf{x}_c,t;\mathbf{D}^*)\geq C_c$, there is no robustness and by convention $\hat{\epsilon}(\mathbf{x}_c,t)=0$.

4. Application

[43] To demonstrate the applicability of the info-gap approach to support decision making in subsurface contaminant remediation, two scenarios will be considered. For both scenarios, two remediation choices are to either remove contaminant mass directly, or increase reaction rate. The performance of the remedial activities is evaluated using an info-gap model that takes into account lack of knowledge about the magnitude of naturally occurring dispersion in the subsurface. Both anthropogenic remedial activities and natural dispersion impact model predicted contaminant concentrations. In the first scenario, the point of compliance is far enough downgradient from the current plume that it will take ~10 years for the concentration peak to pass near the point of compliance. In the second scenario, the point of compliance is much closer to the plume center. It will only take ~1 year for the concentration peak to pass near the point of compliance. These scenarios are consistent with typical site conditions and remedial needs. In many practical situations, the developed relationships can be directly applied by replacing the values for model parameters used below with site-specific data.

4.1. Scenario 1

[44] In this scenario, the fixed parameters are

$$u=30;(\text{m/year}) \tag{24}$$

$$\mathbf{x}_0=(0,0,0);(\text{m}) \tag{25}$$

$$(\sigma_x,\sigma_y,\sigma_z)=(1,1/5,1/20);(\text{m}^2) \tag{26}$$

$$\mathbf{x}_c=(300,50,10);(\text{m}) \tag{27}$$

$$\theta=1/10;(\text{m}^3/\text{m}^3) \tag{28}$$

$$M=1000;(\text{kg}) \tag{29}$$

$$\lambda_0=10^{-2};(1/\text{year}) \tag{30}$$

so that after $t\approx 10;$ (year), the maximum concentrations are observed at the point of compliance. Some or all of the fixed parameters could also be info-gap uncertain and applied in a more complex (likely numerical) info-gap analysis. The dispersion coefficients uncertain and their nominal values are

$$(\tilde{D}_x,\tilde{D}_y,\tilde{D}_z)=(30,7,1/10);(\text{m}^2/\text{year}) \tag{31}$$

[45] The contaminant flow is along the x axis; note the point of compliance is not along the flow path with the peak plume concentrations. Ten years is approximately the time at which robustness is at a minimum, and will therefore be the focus of our attention. The threshold concentration is

$$C_c=25;(\text{g/m}^3) \tag{32}$$

[46] It is assumed that there is a high start-up cost and a low incremental cost for increasing the decay constant λ (relative to the costs for increasing q listed below),

$$S_\lambda=4\times 10^6 \tag{33}$$

$$I_\lambda=10^7 \tag{34}$$

[47] On the other hand, it is assumed that there is no start-up cost and a high incremental cost for additional contaminant-source removal q,

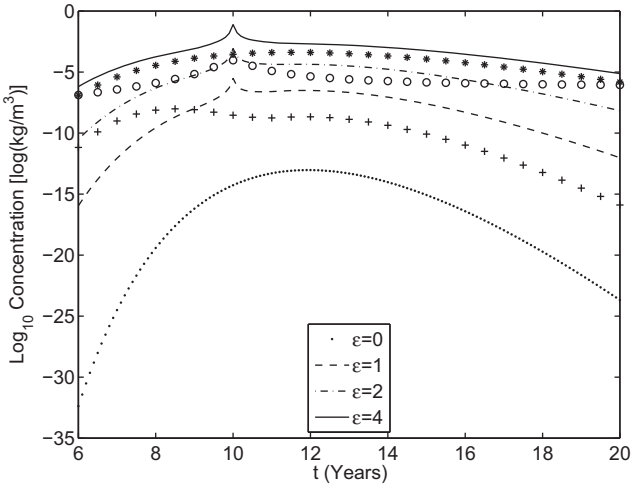

Figure 3. Maximum concentration as a function of time for several horizons of uncertainty (colors) and predicted concentrations for enhanced dispersion (*), heavy-tailed dispersion (°), and a model with a secondary (earlier time arriving and less massive) source (+).

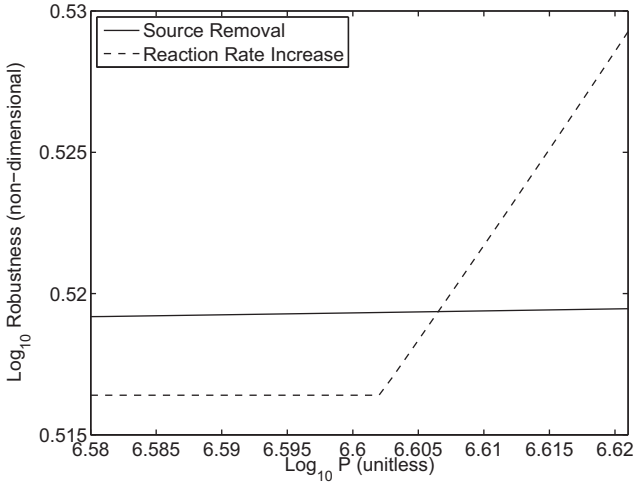

Figure 4. Robustness curves of the two remediation methods at $t = 10$; [year] when the peak concentrations are observed at the point of compliance showing the crossing of the robustness curves.

$$S_q = 0 \tag{35}$$

$$I_q = 10^8 \tag{36}$$

[48] Figure 3 displays the maximum possible concentrations as a function of time for several horizons of uncertainty based on the parameters. $\epsilon = 0$ represents the nominal case; note that maximum concentration is observed at $t \approx 12$; years. For increasing uncertainty horizons ϵ, the maximum concentrations within the info-gap uncertainty bounds are at $t \approx 10$; years which is consistent with the site hydrogeological conditions for Scenario 1 (discussed below). The figure also shows as scatter plots the concentrations for several plausible scenarios based on alternative parameter values of physics-based models. Each of these plausible scenarios are consistent with different uncertainty horizons (Figure 3): enhanced dispersion (*)—consistent with $\epsilon \geq 4$, heavy-tailed dispersion (°)—consistent with $\epsilon \geq 4$, and a model with a secondary (earlier time arriving and less massive) source (+)—consistent with $\epsilon \geq 2$

[49] Figure 4 displays the robustness curves as a function of the remediation budget of each of the two remediation methods near the point where they cross. Figure 5 displays the robustness curves over a larger budget range. Note the robustness curves intersect when $\log_{10} P = \log_{10} P_0 \approx 6.6065$. If the available budget for reducing the contaminant concentrations is less than P_0, source removal is the more robust option. If the available budget is greater than P_0, increasing the reaction rate is more robust. Once P_λ exceeds S_λ, increasing the reaction rate has a strong impact on the robustness. This is not surprising considering that increasing the decay constant decreases the mass exponentially. Given that a relatively long period of time (~10 (year)) passes before the concentration peak passes near the point of compliance, even a small increase in the decay constant can cause a significant decrease in the predicted concentration.

[50] Figure 6 displays the maximum concentration as a function of the horizon of uncertainty for each of the remediation methods at time $t = 10$; (year). In extreme cases with relative error in the dispersion coefficients on the order of 100%, the potential ratio between the transverse and longitudinal dispersivities included in the uncertainty model becomes unrealistically large. This is what causes the sharp rise as $\epsilon \to 1$. For all values of ϵ, increasing the decay constant produces a lower maximum concentration. This is another indication that this is the preferred remediation option with a budget of $P = 10^7$.

[51] Figure 7 displays robustness curves for several different values of P_λ and P_q as a function of time. Note that the robustness reaches a minimum for t near 10; (year) when the highest concentrations are observed at the point of compliance. Increasing spending to increase the decay constant makes a significant increase in the robustness. However, increasing spending to remove more mass has little effect on the robustness in this range of P_q. The plots for

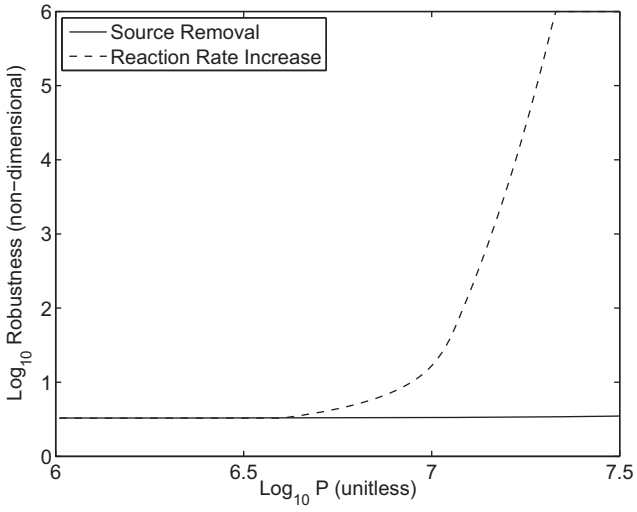

Figure 5. Robustness curves of the two remediation methods at $t = 10$; [year] when the peak concentrations are observed at the point of compliance.

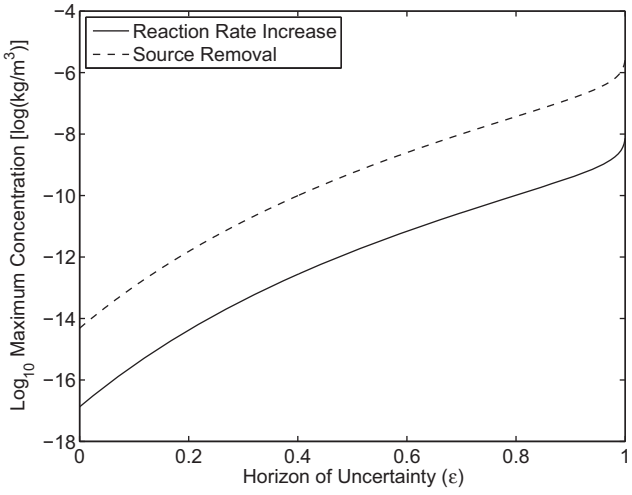

Figure 6. Maximum concentration as a function of the horizon of uncertainty for the two remediation scenarios with $P = 10^7$ at $t = 10$; [year].

P_q nearly sit on top of one another in Figure 7. This provides additional evidence that in this scenario, increasing the decay constant (contaminant reduction rate) is a more robust remediation strategy.

4.2. Scenario 2

[52] This scenario is similar to the previous one, except that the point of compliance is closer to the current plume center, the initial mass is less, and the nominal ambient decay constant (reaction rate) is greater. All nominal and fixed parameters are unchanged except

$$\mathbf{x}_c = (30, 10, 10); [m] \tag{37}$$

$$\lambda_0 = 1; (1/\text{year}) \tag{38}$$

$$M = 100; (\text{kg}) \tag{39}$$

and the cost structure has changed

$$S_\lambda = 8\times10^5 \tag{40}$$

$$I_\lambda = 6\times10^6 \tag{41}$$

$$S_q = 0 \tag{42}$$

$$I_q = 10^7 \tag{43}$$

[53] Note that I_q has decreased by the same factor as M which is in accordance with the concept of there being a fixed incremental cost to remove a unit of mass of the contaminant.

[54] Figure 8 depicts the robustness curves at $t = 1$; (year) for the two remediation strategies as a function of the cost. In this case, the robustness of increasing the reaction rate (decay constant λ) is not as strong as in Scenario 1, largely because there is less time for the reactions to take place before the concentration peak reaches the point of compliance. Another factor in the relative robustness for this scenario is the change in the cost structure. However, unless a very high portion of the mass is removed ($q \rightarrow 1$; larger P_q), the robustness of the two methods as a function of cost is comparable. The preferred remediation method in this case depends strongly on P. For small and large P, source removal provides greater robustness. For intermediate P, increasing the decay constant provides greater robustness. Still, the cost differences are negligible.

[55] Furthering this point is Figure 9 which shows the maximum concentration for the two remediation strategies with $P = 10^{6.9}$ at $t = 1$; (year) as a function of the horizon of uncertainty. The maximum concentrations for the two remediation methods are close at every horizon of uncertainty. When $P = 10^{6.9}$ and $t = 1$; (year), source removal provides greater robustness and a lower maximum concentration, but the differences are not large. Consulting Figure 10, it is seen that increasing the decay constant provides greater robustness at later times, while mass reduction provides greater robustness at early times. This behavior is expected. It demonstrates another important aspect associated with any decision analysis: to take into account time constraints associated with the implementation of the remedial activities. In this case, increased reaction rates take

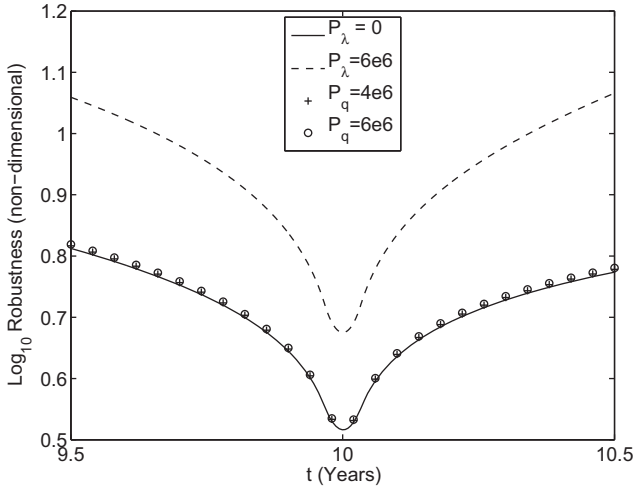

Figure 7. Several robustness curves as a function of time for increasing values of P_λ (solid and dash lines) and P_q (symbols). Note that the lines for increasing P_q fall almost on top of each other.

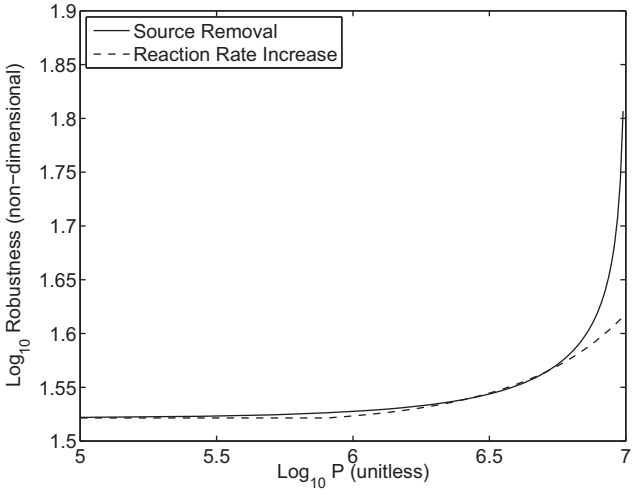

Figure 8. Robustness curves of the two remediation methods at $t = 1$; [year] when the peak concentrations are observed at the point of compliance.

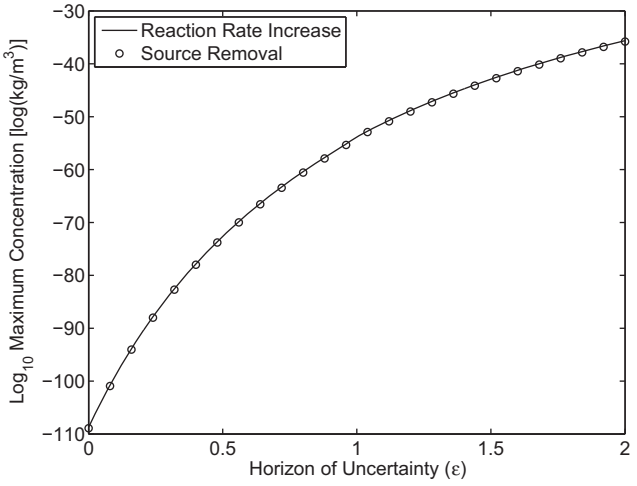

Figure 9. Maximum concentration as a function of the horizon of uncertainty for the two remediation scenarios with $P = 10^{6.9}$ at $t = 1$; [year].

time to improve subsurface conditions. On the other hand, source removal has a more immediate effect. In Scenario 1, time was on the side of increasing the reaction rate. In Scenario 2, time is short enough that source removal becomes a viable option.

5. Discussion

[56] The physics-based model that we have employed here is simple compared to many models that are frequently used in subsurface hydrology. In many cases, a more complex model may be needed, and we wish to provide a perspective on how information gap decision theory (IGDT) can be applied in these cases. The challenges that are likely to arise in the implementation of info-gap for more complex models are primarily computational. For instance, consider a complex numerical model with many parameters (perhaps different dispersion coefficients in a number of different hydrostratigraphic zones, a heterogeneous conductivity field, complex boundary conditions, etc.) Developing an info-gap uncertainty model for these systems can follow the approach we have used here (equation s (15) and (16)). The difference being that equation (15) would consider uncertainty in all the unknown model parameters rather than just the dispersion coefficients, as has been done here. The challenge associated with the added complexity is found in equation (20). For high-dimensional problems, the computation of the robustness function for a series of horizons of uncertainties with different ϵ values will likely not be estimated analytically as it has been here. It may require numerical optimization (maximization) techniques that are computationally efficient, robust, and utilize high-performance computing resources. However, the optimization analyses do not necessitate exploring the whole parameter space constrained by a given horizon of uncertainty. Only regions in the parameter space where the concentrations are the highest need to be identified while regions of intermediate and low concentrations need not be characterized. As a result, the IGDT analyses are expected to be less computationally expensive than, say, a probabilistic technique with a uniform distribution over the parameter space.

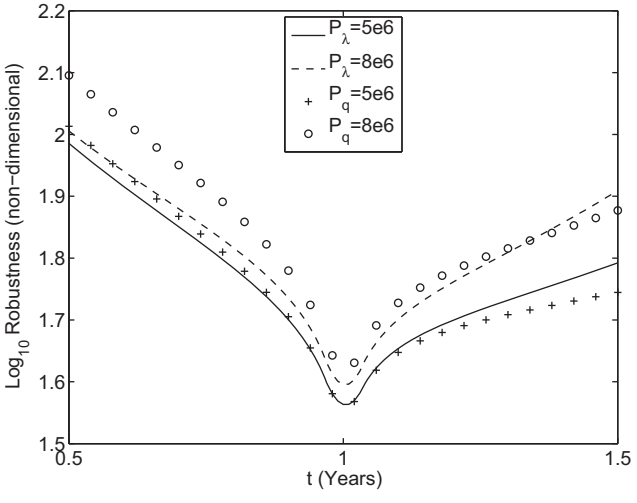

Figure 10. Several robustness curves as a function of time for increasing values of P_λ (solid and dash lines) and P_q (symbols).

6. Conclusion

[57] Decisions related to contaminant remediation are often performed under severe uncertainty. The uncertainties create challenges in predicting future contaminant concentrations which are impacted by naturally occurring processes and remediation activities. Because of this, when designing or deciding between remediation methods within budget constraints, it is prudent to account for these uncertainties. The approach used here is based on the info-gap decision theory which accounts for lack of knowledge in naturally occurring dispersion and the functional form of the transport model. A sequence of info-gap analyses were considered with increasing complexity. The terminal element in this sequence involved an advection-diffusion contaminant spreading model tied to an uncertainty model representing lack of knowledge about the magnitude of contaminant dispersion in the subsurface and the functional form of the transport model. This physics-based model for contaminant concentrations upon which the info-gap uncertainty model is based incorporates the effects of anthropogenic remedial activities and naturally occurring dispersion. The info-gap analysis takes into account this lack of knowledge and how it impacts the design of remedial activities within specific budget constraints. The general approach of the info-gap decision theory is to prefer the remediation method that has the greatest robustness at a fixed cost or the lowest cost at a fixed robustness level. This approach was applied to two different scenarios. In the first, a remediation approach based on increasing the reaction rate was preferred. This was due in large part to the fact that 10; (year) elapsed before the peak contaminant concentrations are observed at the point of compliance. In the other scenario, there was less clarity in the preferred method, and it depended on the monetary price that could be spent on remediation. These scenarios demonstrate that info-gap decision theory provides a viable tool for

supporting decisions related to contaminant remediation taking into account uncertainties and implementation costs.

Appendix A: Maximizing Concentration as a Function of Dispersion Coefficients

[58] Before maximizing equation (14) with respect to the dispersion coefficients, observe that it can be rewritten as a function of the dispersion coefficients

$$C(D_x, D_y, D_z) = A \prod_{w \in \{x,y,z\}} \frac{\exp\left(-\frac{(w-w_0-u_w t)^2}{2(2D_w t+\sigma_w^2)}\right)}{\sqrt{(2D_w t+\sigma_w^2)}} \tag{A1}$$

where A is constant with respect to the dispersion coefficients and $(u_x, u_y, u_z) = (u, 0, 0)$. In order to maximize equation (A1) within the bounds given by equation (15), it is sufficient to maximize

$$f(D_w) = \frac{\exp\left(-\frac{(w-w_0-u_w t)^2}{2(2D_w t+\sigma_w^2)}\right)}{\sqrt{(2D_w t+\sigma_w^2)}} \tag{A2}$$

within the interval $I_\epsilon = [\max\{0, (1-\epsilon)\tilde{D}_w\}, (1+\epsilon)\tilde{D}_w]$. Differentiating with respect to D_w, we obtain

$$f'(D_w) = \frac{te^{-\frac{(w-w_0-u_w t)^2}{2(2D_w t+\sigma_w^2)}}\left((w-w_0-u_w t)^2 - 2D_w t - \sigma_w^2\right)}{(2D_w t+\sigma_w^2)^{5/2}} \tag{A3}$$

[59] Setting this equal to zero and solving (ignoring the case $t = 0$), we obtain

$$D_w^* = \frac{(w-w_0-u_w t)^2 - \sigma_w^2}{2t} \tag{A4}$$

[60] Note that $f'(D_w) > 0$ when $D_w < D_w^*$ and $f'(D_w) < 0$ when $D_w > D_w^*$. Hence, D_w^* is a global maximizer. If $D_w^* \in I_\epsilon$ then the maximum within the interval is obtained when $D_w = D_w^*$. If $D_w^* > (1+\epsilon)\tilde{D}_w^*$ then $f(D_w)$ is increasing on I_ϵ and the maximum is obtained at the right end point. If $D_w^* < \max\{0, (1-\epsilon)\tilde{D}_w^*\}$ then $f(D_w)$ is decreasing on I_ϵ and the maximum is obtained at the left end point. Putting this in symbols,

$$D_w^* = \max\left\{0, (1-\epsilon)\tilde{D}_w, \min\left\{(1+\epsilon)\tilde{D}_w, \frac{(w_c-w_0-u_w t)^2 - \sigma_w^2}{2t}\right\}\right\} \tag{A5}$$

[61] **Acknowledgments.** The authors wish to thank Y. Ben-Haim for helpful discussions in the preparation of this manuscript. The authors also wish to thank the anonymous reviewers who provided useful comments that improved the manuscript. This research was funded by the Environmental Programs Directorate of the Los Alamos National Laboratory; the Advanced Simulation Capability for Environmental Management (ASCEM) project, Department of Energy, Environmental Management; and the Integrated Multifaceted Approach to Mathematics at the Interfaces of Data, Models, and Decisions (DiaMonD) project, Department of Energy, Office of Science.

References

Abbaspour, K. C., M. T. van Genuchten, R. Schulin, and E. Schläppi (1997), A sequential uncertainty domain inverse procedure for estimating subsurface flow and transport parameters, *Water Resour. Res.*, *33*(8), 1879–1892.

Agostini, P., A. Critto, E. Semenzin, and A. Marcomini (2009a), Decision support systems for contaminated land management: A review, in *Decision Support Systems for Risk-Based Management of Contaminated Sites*, pp. 1–20, Springer, N. Y.

Agostini, P., G. W. Suter II, S. Gottardo, and E. Giubilato (2009b), Indicators and endpoints for risk-based decision processes with decision support systems, in *Decision Support Systems for Risk-Based Management of Contaminated Sites*, pp. 1–18, Springer, N. Y.

Argent, R. M., J.-M. Perraud, J. M. Rahman, R. B. Grayson, and G. Podger (2009), A new approach to water quality modelling and environmental decision support systems, *Environ. Modell. Software*, *24*(7), 809–818.

Bedford, T., and R. Cooke (2001), *Probabilistic Risk Analysis: Foundations and Methods*, Cambridge Univ. Press, Cambridge, U. K.

Ben-Haim, Y. (2006), *Info-Gap Decision Theory: Decisions Under Severe Uncertainty*, Elsevier, London.

Beven, K., and I. Westerberg (2011), On red herrings and real herrings: Disinformation and information in hydrological inference, *Hydrol. Processes*, *25*(10), 1676–1680.

Bolster, D., M. Barahona, M. Dentz, D. Fernandez-Garcia, X. Sanchez-Vila, P. Trinchero, C. Valhondo, and D. Tartakovsky (2009), Probabilistic risk analysis of groundwater remediation strategies, *Water Resour. Res.*, *45*, W06413, doi:10.1029/2008WR007551.

Caselton, W. F., and W. Luo (1992), Decision making with imprecise probabilities: Dempster-shafer theory and application, *Water Resour. Res.*, *28*(12), 3071–3083.

Dagan, G. (1982), Stochastic modeling of groundwater flow by unconditional and conditional probabilities: 1. Conditional simulation and the direct problem, *Water Resour. Res.*, *18*(4), 813–833.

Deeb, R., E. Hawley, L. Kell, and R. O'Laskey (2011), Assessing alternative endpoints for groundwater remediation at contaminated sites, technical report, DTIC document, Environmental Security Technology Certification Program (ESTCP), Alexandria, Va.

Delhomme, J. (1979), Spatial variability and uncertainty in groundwater flow parameters: A geostatistical approach, *Water Resour. Res.*, *15*(2), 269–280.

Fox, D. R., Y. Ben-Haim, K. R. Hayes, M. A. McCarthy, B. Wintle, and P. Dunstan (2007), An info-gap approach to power and sample size calculations, *Environmetrics*, *18*(2), 189–203.

Harp, D. R., and V. V. Vesselinov (2013), Contaminant remediation decision analysis using information gap theory, *Stochastic Environ. Res. Risk Assess.*, *27*(1), 159–168.

Hine, D., and J. W. Hall (2010), Information gap analysis of flood model uncertainties and regional frequency analysis, *Water Resour. Res.*, *46*, W01514, doi:10.1029/2008WR007620.

Hipel, K. W., and Y. Ben-Haim (1999), Decision making in an uncertain world: Information-gap modeling in water resources management, *Syst. Man Cybern.*, *29*(4), 506–517.

Jordan, G., and A. Abdaal (2013), Decision support methods for the environmental assessment of contamination at mining sites, *Environ. Monit. Assess.*, *185*(9), 7809–7832, doi:10.1007/s10661-013-3137-z.

Keating, E. H., J. Doherty, J. A. Vrugt, and Q. Kang (2010), Optimization and uncertainty assessment of strongly nonlinear groundwater models with high parameter dimensionality, *Water Resour. Res.*, *46*, W10,517, doi:10.1029/2009WR008584.

Laloy, E., and J. A. Vrugt (2012), High-dimensional posterior exploration of hydrologic models using multiple-try dream (zs) and high-performance computing, *Water Resour. Res.*, *48*, W01526, doi:10.1029/2011WR010608.

Levy, J. K., K. W. Hipel, and D. M. Kilgour (2000), Using environmental indicators to quantify the robustness of policy alternatives to uncertainty, *Ecol. Modell.*, *130*(1), 79–86.

McCarthy, M. A., and D. B. Lindenmayer (2007), Info-gap decision theory for assessing the management of catchments for timber production and urban water supply, *Environ. Manage.*, *39*(4), 553–562.

Montanari, A., C. A. Shoemaker, and N. van de Giesen (2009), Introduction to special section on uncertainty assessment in surface and subsurface hydrology: An overview of issues and challenges, *Water Resour. Res.*, *45*, W00B00, doi:10.1029/2009WR008471.

Morales-Casique, E., S. P. Neuman, and V. V. Vesselinov (2010), Maximum likelihood Bayesian averaging of airflow models in unsaturated fractured tuff using Occam and variance windows, *Stochastic Environ. Res. Risk Assess.*, *24*(6), 863–880.

Neuman, S. (2003), Maximum likelihood bayesian averaging of uncertain model predictions, *Stochastic Environ. Res. Risk Assess.*, *17*(5), 291–305.

NRC, U. N. R. C. (1999), *An End State Methodology for Identifying Technology Needs for Environmental Management, With an Example From the Hanford Site Tanks*, Natl. Acad. Press, Washington, D. C.

NRC, U. N. R. C. (2013), *Alternatives for Managing the Nation's Complex Contaminated Groundwater Sites*, Natl. Acad. Press, Washington, D. C.

Pierce, E. M., et al. (2009), *Scientific Opportunities to Reduce Risk in Groundwater and Soil Remediation*, Pac. Northwest Natl. Lab, Springfield, Va.

Reeves, D. M., K. F. Pohlmann, G. M. Pohll, M. Ye, and J. B. Chapman (2010), Incorporation of conceptual and parametric uncertainty into radionuclide flux estimates from a fractured granite rock mass, *Stochastic Environ. Res. Risk Assess.*, *24*(6), 899–915.

Rügner, H., M. Finkel, A. Kaschl, and M. Bittens (2006), Application of monitored natural attenuation in contaminated land management—A review and recommended approach for Europe, *Environ. Sci. Policy*, *9*(6), 568–576.

Singh, A., S. Mishra, and G. Ruskauff (2010), Model averaging techniques for quantifying conceptual model uncertainty, *Ground Water*, *48*(5), 701–715.

Tartakovsky, D. M. (2007), Probabilistic risk analysis in subsurface hydrology, *Geophys. Res. Lett.*, *34*, L05404, doi:10.1029/2007GL029245.

Tonkin, M., and J. Doherty (2009), Calibration-constrained Monte Carlo analysis of highly parameterized models using subspace techniques, *Water Resour. Res.*, *45*, W00B10, doi:10.1029/2007WT006678.

Wagner, B. J., and S. M. Gorelick (1987), Optimal groundwater quality management under parameter uncertainty, *Water Resour. Res.*, *23*(7), 1162–1174.

Wang, H., and H. Wu (2009), Analytical solutions of three-dimensional contaminant transport in uniform flow field in porous media: A library, *Frontiers Environ. Sci. Eng. China*, *3*(1), 112–128.

Ye, M., S. P. Neuman, and P. D. Meyer (2004), Maximum likelihood Bayesian averaging of spatial variability models in unsaturated fractured tuff, *Water Resour. Res.*, *40*, W05113, doi:10.1029/2003WR002557.